PIERRE WELANDER

School of Oceanography, University of Washington, Seattle, WA 98195 (U.S.A.)

(Received March 3, 1981; revised and accepted November 16, 1981)

ABSTRACT

Welander, P., 1982. A simple heat–salt oscillator. Dyn. Atmos. Oceans, 6: 233–242.

A theoretical study is made of a simple mixed-layer model, in the form of a well-mixed constant-depth layer, forced from above by a heat flux $k_T(T_A - T)$ and salinity flux $k_S(S_A - S)$, where T_A and S_A are two reference values and T and S the temperature and salinity of the layer. The layer has a turbulent exchange of heat and salt with underlying water, kept at constant temperature and salinity, which is small in a statically stable case; large in a statically unstable case. If $k_T > k_S$, self-sustained oscillations may occur. In one cycle, a fast temperature rise, a slower salinity increase, and a final relaxation when the layer adjusts to the conditions of the underlying water, are observed.

1. INTRODUCTION

Water stratified by heat and salt can become unstable because of the difference in molecular diffusivity for heat and salt (see Turner, 1973, for a review of these double-diffusive phenomena). It can be asked whether similar instabilities may occur in a well-mixed water body that is subjected to an external thermohaline forcing, with fluxes given by a linear Newtonian law, where the corresponding adjustment times for temperature and salinity are different. Stommel (1961) has studied a simple box model comprising two or more well-mixed water reservoirs with advective coupling, forced in the way described. He finds that when $k_T \neq k_S$, multiple steady states may appear. However, the system always goes to a stable steady state.

The author has considered a different, simple model which involves a single well-mixed water layer of fixed depth, overlying a water reservoir of given temperature T_0 and salinity S_0 (Fig. 1). Turbulent fluxes of heat and salt, according to a Newtonian transfer law, occur between these two water bodies, with the transfer coefficient k dependent on the density difference, $\Delta\rho = \rho - \rho_0$: k is small for negative $\Delta\rho$, but increases rapidly as $\Delta\rho$ becomes positive.

0377-0265/82/0000–0000/$02.75

This system may become unstable, and go into self-sustained oscillations, if the response time associated with the external forcing is larger for the temperature than for the salinity. The aim of this paper is to demonstrate

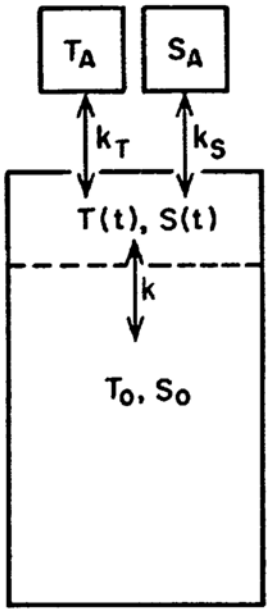

Fig. 1. The basic model. The values T_A and S_A are the effective temperature and salinity of the external forcing; T_0 and S_0 are the temperature and salinity of the deep reservoir; and k_T, k_S and k are the coefficients in assumed Newtonian-type transfer laws.

this phenomenon in one example. Whether the oscillation occurs in the real world depends critically on the shape of the function $k(\Delta\rho)$. This shape depends on the turbulent mechanism and how this is affected by the static stability. The difficulty of predicting $k(\Delta\rho)$ theoretically is obvious. However, in a controlled laboratory experiment, where the turbulence is generated by a stirrer, $\Delta\rho$ may be varied and the curve $k(\Delta\rho)$ determined experimentally. Presumably, experiments could be arranged which generate forms for $k(\Delta\rho)$ of a type allowing self-sustained oscillations, but this remains to be proved.

In real oceanic mixed layers some of the conditions for an oscillation appear to be fulfilled. The adjustment time for salinity is long compared to that of temperature. In fact, the salinity flux is almost independent of S, corresponding to the limit $k_S \to 0$, $S_A \to \infty$ in our model. However, the exchange between the mixed layer and the underlying water is not as simple

as in the model: it is associated with erosions of a basic statically stable density profile, and is further complicated by Ekman up- and down-wellings. Nevertheless, it may be worthwhile to look for special situations in the oceans where conditions appear favorable for an oscillatory overturning of the type demonstrated by the present, simple model.

2. MODEL EQUATIONS AND THE STEADY STATE

With reference to Fig. 1. and the general description of the model given in the previous section, the following equations can be formulated:

$$\dot{T} = k_T(T_A - T) - k(\rho)T \tag{1}$$

$$\dot{S} = k_S(S_A - S) - k(\rho)S \tag{2}$$

$$\rho = -\alpha T + \gamma S \tag{3}$$

where, for simplicity, we have set $T_0 = S_0 = \rho_0 = 0$. The equation of state is linear, k_T and k_S are constants, and $k(\rho)$ is a positive function, monotonically increasing with ρ. Since the exchange between the layer and the reservoir is assumed fully turbulent, the same coefficient k is used for both heat and salt.

The steady state, denoted by $\bar{T}$, $\bar{S}$ and $\bar{\rho}$, is found from the equations

$$\bar{T} = \frac{k_T T_A}{k_T + \bar{k}}, \quad \bar{S} = \frac{k_S S_A}{k_S + \bar{k}} \tag{4,5}$$

$$\bar{\rho} = -\alpha\bar{T} + \gamma\bar{S} = \frac{-k_T \alpha T_A}{k_T + \bar{k}} + \frac{k_S \gamma S_A}{k_S + \bar{k}} = F(\bar{\rho}) \tag{6}$$

where $\bar{k}$ means $k(\bar{\rho})$. The value $\bar{\rho}$ is (implicitly) determined by eq. 6;

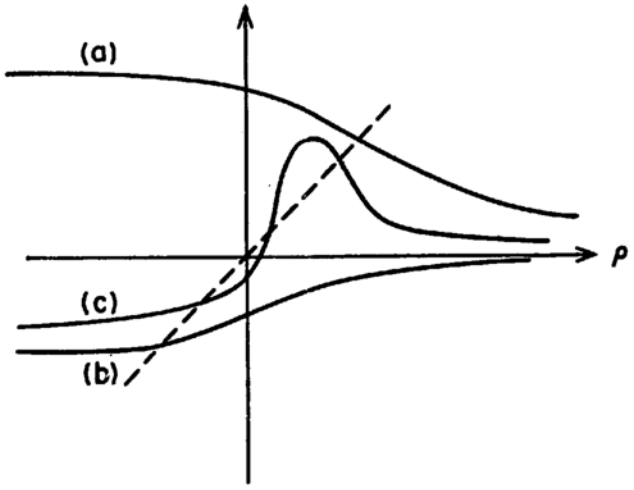

Fig. 2. Examples of possible forms for $F(\rho)$ in a case where $k(\rho)$ increases monotonically. In the cases (a) and (b) there exists one steady state, in the case (c), three steady states.

knowing $\bar{\rho}$ the values $\bar{T}$ and $\bar{S}$ can be obtained from (4, 5).

There may be one, or several (an odd number) steady states. This should be obvious from Fig. 2, which shows the general curve-shapes for $F(\bar{\rho})$ which can be generated by a $k(\bar{\rho})$ curve of the assumed type.

For simplicity, the case of a single steady state is considered. From Fig. 2, it can be seen that this case occurs if $F'(\bar{\rho}) < 1$. This condition takes the form

$$\left[\frac{k_T \alpha T_A}{(k_T + \bar{k})^2} - \frac{k_S \gamma S_A}{(k_S + \bar{k})^2}\right] \bar{k}' < 1 \tag{7}$$

where $\bar{k}'$ means $k'(\bar{\rho})$. The inequality is satisfied if

$$\frac{k_T \alpha T_A}{(k_T + \bar{k})^2} < \frac{k_S \gamma S_A}{(k_S + \bar{k})^2} \tag{7a}$$

or, if this condition is not met, if

$$\bar{k}' < \left[\frac{k_T \alpha T_A}{(k_T + \bar{k})^2} - \frac{k_S \gamma S_A}{(k_S + \bar{k})^2}\right]^{-1} \tag{7b}$$

3. STABILITY OF THE STEADY STATE

The stability of the steady state is studied by setting $T = \bar{T} + \theta$, $S = \bar{S} + \sigma$ and $\rho = \bar{\rho} + q$, and examining eqs. 1, 2 and 3 in the limit of small θ, σ and q. We find the perturbation equations

$$\dot{\theta} = -(k_T + \bar{k})\theta - \bar{k}'\bar{T}q \tag{8}$$

$$\dot{\sigma} = -(k_S + \bar{k})\sigma - \bar{k}'\bar{S}q \tag{9}$$

$$q = -\alpha\theta + \gamma\sigma \tag{10}$$

This leads to the system

$$\begin{aligned} &\dot{\theta} + a\theta + b\sigma = 0 \\ &\dot{\sigma} + c\sigma + d\theta = 0 \end{aligned} \tag{11}$$

where

$$\begin{aligned} a &= k_T + \bar{k}_S - \bar{k}'\alpha\bar{T} \\ b &= \bar{k}'\gamma\bar{T} \\ c &= k_S + \bar{k} + \bar{k}'\gamma\bar{S} \\ d &= -\bar{k}'\alpha\bar{S} \end{aligned} \tag{12}$$

If at least one of the terms $a + c$ and $ac - bd$ is negative, the system (11)

has a solution of the form $e^{\lambda t}$ with Re $\lambda > 0$, i.e., an unstable solution. The condition $ac - bd < 0$ leads to a condition that is the converse of (7), i.e., $F'(\bar{\rho}) > 1$, and there must exist several steady states. It is therefore assumed that $a + d < 0$, which condition reads

$$k_T + k_S + 2\bar{k} + \bar{\rho}\bar{k}' < 0 \tag{13}$$

As $\bar{k} > 0$, $\bar{k}' > 0$ is assumed, it is necessary that $\bar{\rho} < 0$, i.e., the steady state must be statically stable. It can be shown that the two conditions (7) and (13) further require that $k_T > k_S$; an inequality already assumed.

As will be demonstrated in Section 5, functions $k(\rho)$ and sets of parameter values k_T, k_S, α, γ, T_A and S_A can be found, that satisfy the foregoing conditions for a single, unstable steady state. Since the system is autonomous second order, with no trajectories in an S-T-plane escaping to infinity, such an unstable steady state must necessarily lead to a single-periodic self-sustained oscillation (a limit cycle in the T-S-plane).

4. THE FLIP-FLOP MODEL

A simple limiting variant of the model described is obtained by taking $k(\rho)$ as a step function

$$\begin{aligned} k &= k_0 \quad \rho \leqslant -\epsilon \\ k &= k_1 \quad \rho > -\epsilon \end{aligned} \tag{14}$$

where k_0 is a small constant or zero, k_1 is a large constant, and ϵ is a small, positive constant.

The flip-flop model has two steady states

$$\bar{T} = \frac{k_T T_A}{k_T + k_0}, \; \bar{S} = \frac{k_S S_A}{k_S + k_0}, \text{ if } \bar{\rho} \leqslant -\epsilon \tag{15a}$$

$$\bar{T} = \frac{k_T T_A}{k_T + k_1}, \; \bar{S} = \frac{k_S S_A}{k_S + k_1}, \text{ if } \bar{\rho} > -\epsilon \tag{15b}$$

If $\bar{\rho} \leqslant -\epsilon$, we find $\bar{T} \approx T_A$ and $\bar{S} \approx S_A$, since k_0 is assumed to be small. If $\gamma S_A > \alpha T_A$ this steady state can never be reached. Similarly, if $\bar{\rho} > -\epsilon$, $\bar{T} \approx k_T/k_1 \cdot T_A$ and $\bar{S} \approx k_S/k_1 \cdot S_A$, since k_1 is large; and if $\bar{\rho} < -\epsilon$ and k_T/k_S is large enough, again the steady state cannot be reached. These steady states act as two "attractors" for the phase-plane trajectories, causing an oscillatory solution (Fig. 3).

The exact condition for the non-existing steady states reads

$$\frac{-k_T \alpha T_A}{k_T + k_1} + \frac{k_S \gamma S_A}{k_S + k_1} < -\epsilon < \frac{-k_T \alpha T_A}{k_T + k_0} + \frac{k_S \gamma S_A}{k_S + k_0} \tag{16}$$

There always exists a range of possible values for $\alpha T_A / \gamma S_A$ satisfying this

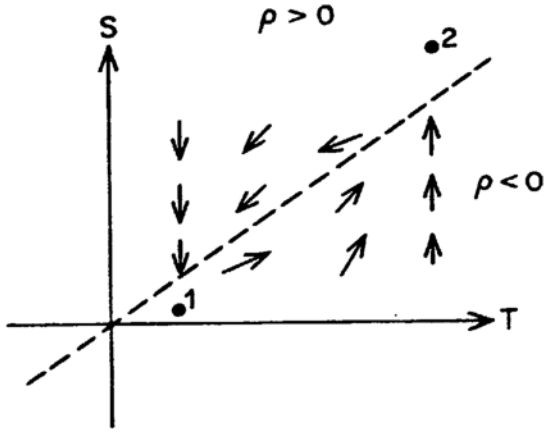

Fig. 3. Schematic picture of the flip-flop model in a T-S-plane. The points 1 and 2 represent the non-existing steady states which act as "attractors" when the solution point is in the half-plane $\rho \leqslant -\epsilon$ and $\rho > -\epsilon$, respectively. The slope dS/dT has a discontinuity at the line $\rho = -\epsilon$.

condition when $k_1 > k_0$ and $k_T > k_S$, as has been assumed.

The present flip-flop model is a degenerate variant of the general model described in Section 2. In a corresponding continuous version, with a function $k(\rho)$ approaching a step-function, there may be one or several steady states. The behavior of the system near these states obviously cannot be deduced from the flip-flop model. However, existing finite-amplitude self-sustained oscillations can be explored, at least qualitatively, by this model.

The reader may wonder why the step is placed at $\rho = -\epsilon$ rather than at $\rho = 0$. The answer is that solutions in the second case always show a decay, sometimes very gradual (which means that if a numerical integration method is used one must be careful not to produce false limit cycles). There is no steady state, but a pseudo-steady state is approached. This pseudo-steady state is characterized by a vibration of the system which increases in frequency, to infinite values, as the amplitude decreases, and obviously is an effect of the discontinuity in k.

5. TWO NUMERICAL EXAMPLES

Consider two specific, numerical examples; in the first example the function $k(\rho)$ is continuous and of the form

$$k(\rho) = 2k_1/\pi[\arctan m(\rho + \rho_1) + \pi/2] \tag{17}$$

This function is positive and increases monotonically from 0 to k_1, when ρ increases from $-\infty$ to $+\infty$. There is no special physical reason for choosing this form, we merely want to demonstrate the oscillation in one example that

is mathematically simple to analyze. The parameter values chosen are

$$\frac{\alpha T_A}{\gamma S_A} = \frac{4}{5},\ \frac{k_T}{k_S} = 2,\ \frac{k_1}{k_T} = \frac{1}{2},\ \frac{\rho_1}{\gamma S_A} = \frac{1}{30} \text{ and } m\gamma S_A = 625$$

In this case, there is a steep increase in k near $\rho = 0$. Using non-dimensional variables

$$T^* = \frac{T}{T_A},\ S^* = \frac{S}{S_A},\ \rho^* = \frac{\rho}{\gamma S_A} \text{ and } t^* = k_T t,$$

eqs. 1, 2 and 3 become

$$\dot{T}^* = 1 - T^* - k^*(\rho^*)T^* \tag{18}$$

$$\dot{S}^* = 0.5(1 - S^*) - k^*(\rho^*)S^* \tag{19}$$

$$\rho^* = -0.8T^* + S^* \tag{20}$$

where

$$k^*(\rho^*) = \frac{1}{\pi} \arctan\left(500\rho^* + \frac{50}{3} + \frac{\pi}{2}\right) \tag{21}$$

and the dot means $\mathrm{d}/\mathrm{d}t^*$. The system has a single steady state,

$$\bar{T}^* = \frac{2}{3},\ \bar{S}^* = \frac{1}{2},\ \bar{\rho}^* = -\frac{1}{30}$$

that is found to be unstable by the criterion (13). The resulting self-sustained

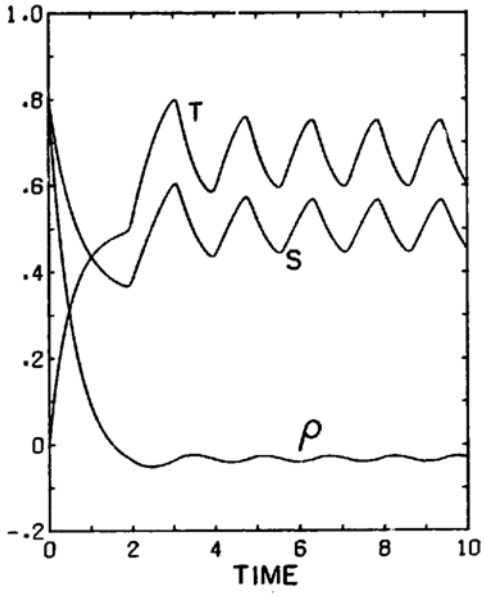

Fig. 4. The solution $T(t)$ and $S(t)$ through a few cycles in the first numerical example described in Section 5. This solution was obtained by step-by-step numerical integration using the Runge-Kutta method.

oscillation, which is reached from all initial states, is depicted in Fig. 4. The calculation was made by step-by-step numerical integration on a programmable calculator (HP 97) and checked by a more accurate calculation using the CDC 6400 computer at the University of Washington.

In the second example, k is discontinuous (the flip-flop model), with the choice of parameters

$$\frac{\alpha T_A}{\gamma S_A} = 0.2,\ \frac{k_T}{k_S} = 10,\ \frac{k_0}{k_T} = 0,\ \frac{k_1}{k_T} = 5 \text{ and } \frac{\epsilon}{\gamma S_A} = -0.01.$$

The corresponding non-dimensional equations are

$$\dot{T}^* = 1 - T^* - \begin{pmatrix} 0 \\ 5 \end{pmatrix} T^* \tag{22}$$

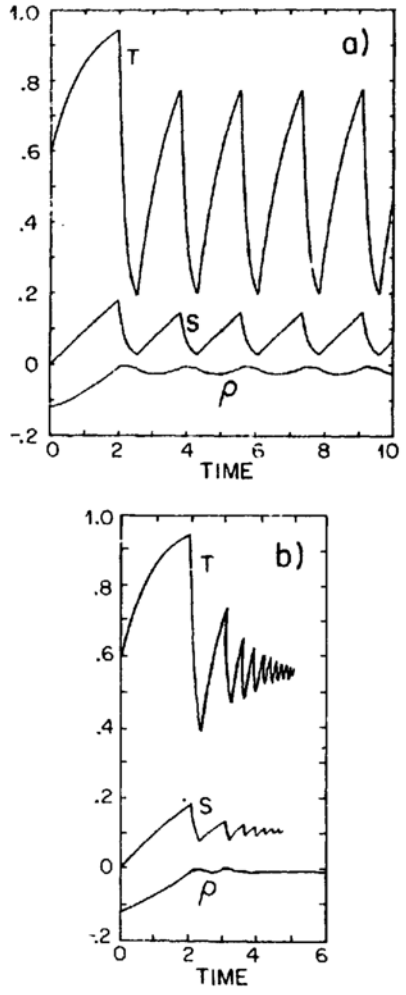

Fig. 5. (a) The solution $T(t)$ and $S(t)$ through a few cycles in the second numerical example described in Section 5 (the flip-flop case). The solution was obtained by numerical joining of two exponential solutions. (b) The solution when $\epsilon = 0$, other parameters unchanged.

$$\dot{S}^* = 0.1(1 - S^*) - \begin{pmatrix} 0 \\ 5 \end{pmatrix} S^* \tag{23}$$

$$\rho^* = -0.2T^* + S^* \tag{24}$$

with the upper value in the bracket applying when $\rho^* \leqslant -0.01$, the lower when $\rho^* > -0.01$. The solution curve, calculated on an HP 97 and checked by numerical integration using the CDC 6400 computer, is shown in Fig. 5a. Finally, the same calculation is repeated with

$$\frac{\epsilon}{\gamma S_A} = 0$$

the other parameters are as before. In this case the approach to the pseudo-steady state mentioned in the previous section is observed (Fig. 5b).

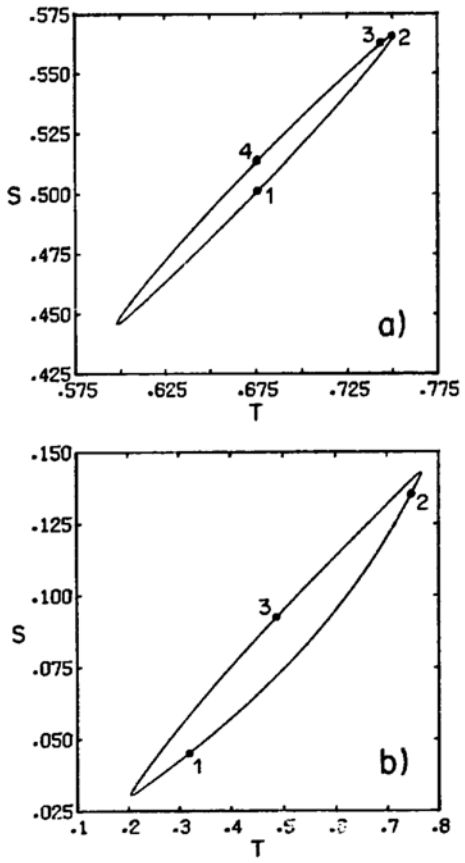

Fig. 6. Phase-plane pictures of the oscillation shown in Fig. 4 (case a) and Fig. 5a (case b). The numbers refer to points discussed in Section 6.

6. PHYSICAL PICTURE OF THE OSCILLATION

The oscillation produced in the example with a continuous $k(\rho)$-function (Fig. 4) is almost harmonic, with a phase-plane picture resembling an ellipse (Fig. 6a). The motion of a point in this phase-plane picture can be followed, and the forcings that move it checked. Starting at a point where $T = \bar{T}$ and $S < \bar{S}$, (Fig. 6a, point 1), T will increase because $\rho < \bar{\rho}$ and $k < \bar{k}$, producing an unbalanced positive part of the forcing term $-kT$ in eq. 1. Since $S < \bar{S}$ and $\rho < \bar{\rho}$, S must also increase. When T becomes larger than $\bar{T}$, a negative restoring force appears, this is large because k_T is large. Thus T will eventually decrease with S still increasing, since k_S is small (point 2). The phase difference between T and S, although small, can be traced in Fig. 4. With T decreasing and S increasing the density increases, and eventually $\rho > \bar{\rho}$ (point 3). All forcings now become negative and both T and S decrease. When T reaches $\bar{T}$, S is still above $\bar{S}$ (point 4), and $\rho > \bar{\rho}$ and $k > \bar{k}$. The second half of the cycle can be discussed by arguments along a similar line, and are not given here.

The larger amplitude oscillations exhibited by the flip-flop model solution has the phase-plane curve shown in Fig. 6b. Starting in a situation where T and S are small and $\rho < -\epsilon$ (Fig. 6b, point 1), both T and S increase, but T increases faster because k_T is large. After some time, T lies close to $\bar{T}_2$, the temperature of "attractor point" 2 in Fig. 3, with S increasing (point 2). Eventually, the line $\rho = -\epsilon$ is passed, and the large restoring terms $-k_1 T$ and $-k_1 S$ make T and S collapse (point 3). The phase-plane point, moving toward the "attractor point" 1 in Fig. 3, will eventually cross the line $\rho = -\epsilon$, and the cycle is repeated.

ACKNOWLEDGMENTS

The author thanks Bruce Long for help with some of the numerical calculations. Part of the work was carried out during the author's visit to the Max-Planck-Institute for Meteorology in Hamburg. Support for the work has been given by the National Science Foundation through grant number OCE80-07927. The paper represents contribution number 1260 from the School of Oceanography, University of Washington, Seattle, WA 98195.

REFERENCES

Stommel, H., 1961. Thermohaline convection with two stable regimes of flow. Tellus, 13: 224–230.

Turner, J.S., 1973. Buoyancy Effects in Fluids, Cambridge University Press, 368 pp.